Article

Not peer-reviewed version

Targeting Skin Aging at Multiple Fronts: Antioxidant, Antielastase, Anticollagenase, and UVB-Protective Effects of *Vitex trifolia*

Donna Maretta Ariestanti *, Pietradewi Hartrianti, Chelsea Clarisa, Farras Kayla Thallah Widodo, Novita Dwi Lestari, Lawrence Mario Wirawan, Redhalfi Fadhila, Abdul Mun'im, Richard Johari James, Syariful Mubarok, Choo Chee Yan, Erika Chriscensia

Posted Date: 24 November 2025

doi: 10.20944/preprints202511.1814.v1

Keywords: *Vitex trifolia*; antioxidant activity; elastase and collagenase inhibition; UVB-induced skin aging

 doi:10.20944/preprints202511.1814.v1

Article

Targeting Skin Aging at Multiple Fronts: Antioxidant, Antielastase, Anticollagenase, and UVB-Protective Effects of *Vitex trifolia*

Donna Maretta Ariestanti [1,*], Pietradewi Hartrianti [2], Chelsea Clarisa [2], Farras Kayla Thallah Widodo [1], Novita Dwi Lestari [2], Mario Lawrence Wirawan [2], Redhalfi Fadhila [1], Abdul Mun'im [1], Richard Johari James [3,4], Syariful Mubarok [5], Choo Chee Yan [4] and Erika Chriscensia [2]

[1] Faculty of Pharmacy, Universitas Indonesia, Depok 16424, Indonesia
[2] I3L University, East Jakarta 13210, Jakarta, Indonesia
[3] Integrative Pharmacogenomics Institute, Universiti Teknologi MARA, Bandar Puncak Alam 42300, Selangor, Malaysia
[4] Faculty of Pharmacy, Universiti Teknologi MARA, Bandar Puncak Alam 42300, Selangor Malaysia
[5] Department of Agronomy, Faculty of Agriculture, Universitas Padjadjaran, Bandung, Indonesia
* Correspondence: donnam.ariestanti@farmasi.ui.ac.id; Tel.: +62 821-2560-3624

Abstract

Skin aging is driven by oxidative stress, extracellular matrix degradation, and UVB-induced cellular injury. Plant-derived bioactives with multi-targeted protective actions offer promising avenues for cosmeceutical development. This study assessed ethanolic leaf extracts of *Vitex trifolia*, an Indonesian medicinal plant traditionally used for skin disorders. Phytochemical analysis showed a total phenolic content of 78.52 ± 0.01 mg GAE/g and total flavonoid content of 1.99 ± 0.02 mg QE/g. LC–HRMS profiling identified major metabolites including casticin and several flavonoid and phenolic acid derivatives. Antioxidant assays demonstrated strong radical-scavenging and reducing activities, with IC_{50} value of 63.47 ± 0.24 (DPPH) and 70.13 ± 1.28 µg/mL (ABTS), and a FRAP value of 36.3 ± 0.18 $FeSO_4$ eq/100 g. Enzymatic studies confirmed potent collagenase inhibition (IC_{50}=27.94 ± 3.20 µg/mL) and moderate elastase inhibition. In HaCaT keratinocytes, *V. trifolia* extract remained non-toxic up to 100 µg/mL and exerted cytoprotective activity against UVB-induced damage at 12.5–50 µg/mL. The extract also downregulated UVB-induced MMP-1 and MMP-9 expression up to 42% and 69%, respectively, outperforming ascorbic acid. These findings highlight *V. trifolia* as a promising natural anti-aging agent with strong antioxidant, protease-inhibitory and photoprotective properties, supporting its potential as safe and effective cosmeceutical ingredient.

Keywords: *Vitex trifolia*; antioxidant activity; elastase and collagenase inhibition; UVB-induced skin aging

1. Introduction

Human skin represents a highly interactive barrier tissue in which genetically programmed senescence intersects with external environmental stressors to shape the aging trajectory [1,2]. Among these external stressors, ultraviolet B (UVB, 280–320 nm) is particularly deleterious, driving molecular alterations that prematurely remodel skin structure and function [3]. Upon UVB exposure, keratinocytes generate bursts of reactive oxygen species (ROS) that exceed intrinsic antioxidant capacity, resulting in oxidative injury to genomic DNA, structural proteins, and membrane lipids [4]. The long-term accumulation of such oxidative insults is clinically reflected in photoaging hallmarks such as deep wrinkles, uneven pigmentation, and gradual decline in skin resilience [5].

 doi:10.20944/preprints202511.1814.v1

Photoaging advances through a two-pronged mechanism: direct oxidative disruption of cellular macromolecules and enzymatic degradation of the extracellular matrix (ECM). ROS-driven activation of elastase leads to fragmentation of elastin fibers, while collagenase progressively dismantles collagen scaffolds—together producing dermal thinning and structural deterioration that visibly accelerate skin aging [6]. Targeting these proteases is therefore a pivotal intervention point. Polyphenol-rich phytochemicals constitute a natural defense strategy, acting dually as potent radical scavengers and as inhibitors of matrix-degrading proteases including elastase and collagenase. Increasing evidence highlights their ability to modulate multiple molecular pathways simultaneously, establishing a rational basis for phytochemical-derived cosmeceuticals [1]. Specifically, ROS could induce the upregulation of matrix metalloprotease 1 (MMP-1) and MMP-9 through the mitogen-activated protein kinase (MAPK) pathway [7]. The upregulation of the MMP-1 and MMP-9 expressions responsible for collagen degradation leads to loss of skin elasticity and presence of wrinkles [8,9]. These mechanistic insights highlight the growing importance of exploring traditional medicinal plants as promising sources of multi-targeted anti-aging compounds.

The global interest in safe, natural skin-care agents has intensified research into botanicals with established ethnomedicinal applications. *Vitex trifolia* L. (legundi) is widely used traditional plants recognized in various Asian systems of medicine for treating inflammatory and dermatological conditions [10,11]. *V. trifolia* is enriched in vitexicarpin, gallic acid, and isovitexin [12]. While these phytoconstituents are acknowledged for their antioxidant, anti-inflammatory, and enzyme-modulating actions, rigorous experimental validation of their anti-aging potential remains scarce.

Despite the accumulating literature on plant polyphenols, gaps persist in understanding the integrated bioactivity profiles of traditional species. Prior studies often focus narrowly on single antioxidant assays or isolated enzyme inhibition, without addressing the combined cellular and biochemical responses under UV-induced stress [1,13]. Moreover, indigenous species with long-standing ethnomedicinal use in Southeast Asia remain underexplored as cosmeceutical candidates [14]. Addressing these gaps requires standardized extraction, quantitative phytochemical characterization, and multi-level assays to bridge traditional claims with modern biomedical validation [15].

Here, we present a systematic investigation into the cosmeceutical potential of *V. trifolia*. Ethanolic extracts were prepared using ultrasonic-assisted extraction and microwave-assisted extraction (MAE), followed by phytochemical quantification, antioxidant profiling, elastase and collagenase inhibition kinetics, and UVB-induced cytoprotection in HaCaT keratinocytes as well as gene expression analysis of MMP-1 and MMP-9. By interrogating oxidative stress cascades, protease-mediated matrix degradation, cellular photodamage, and modulation of MMP-1 and MMP-9 genes, this study provides foundational evidence for developing natural anti-aging cosmeceuticals derived from biodiversity. This study provides the first integrated evaluation of *V. trifolia* for cosmetic use, encompassing phytochemical characterization, antioxidant profiling, elastase and collagenase inhibition, and UVB-induced cytoprotection in HaCaT keratinocytes, providing a holistic view of their skin-protective potential.

2. Results

2.1. Extract Characterisation

The extraction of *V. trifolia* yielded 31.8%, suggesting a high abundance of ethanol-soluble phytochemicals suitable for further chemical and biological evaluation. The total flavonoid content (TFC) and total phenolic content (TPC) of the extract were measured and recorded in Table 1. The total flavonoid content (TFC) and total phenolic content (TPC) were quantified using the $AlCl_3$ and Folin–Ciocalteu methods, respectively (Table 1). The extract contained 1.99 ± 0.02 mg QE/g extract of flavonoids and 78.52 ± 0.01 mg GAE/g extract of phenolic compounds, indicating a phytochemical profile dominated by polyphenolic constituents.

 doi:10.20944/preprints202511.1814.v1

Table 1. Total flavonoid, phenolic content and yield of *V. trifolia* extract

Total flavonoid content (mg QE/g extract)	Total phenolic content (mg GAE/g extract)	Yield (%)
1.99 ± 0.02	78.52 ± 0.01	31.8

QE: quercetin; GAE: gallic acid

Furthermore, to further elucidate its chemical composition, LC–HRMS analysis was performed on the ethanolic extract of *V. trifolia*. LC–HRMS profiling uncovered a remarkably rich metabolite landscape in *V. trifolia* ethanolic extract, with ten major bioactive compounds dominating the chemical profile (Figure 1). Notably, the methylated flavonoid casticin emerged as the predominant metabolite (AUC 2.38 × 10^9), accompanied by an impressive array of glycosylated and polyhydroxylated flavonoid derivatives, modifications known to enhance bioavailability and therapeutic potential. The extract also yielded phenolic acids (4-coumaric acid and 4-hydroxybenzoic acid) with established antioxidant properties, alongside valuable terpenoids including lupeol, a pentacyclic triterpenoid with documented anti-inflammatory activity (Table 2). This exceptional concentration of bioactive polyphenols and terpenoids establishes *V. trifolia* as a promising source of structurally diverse natural products with potential pharmaceutical applications.

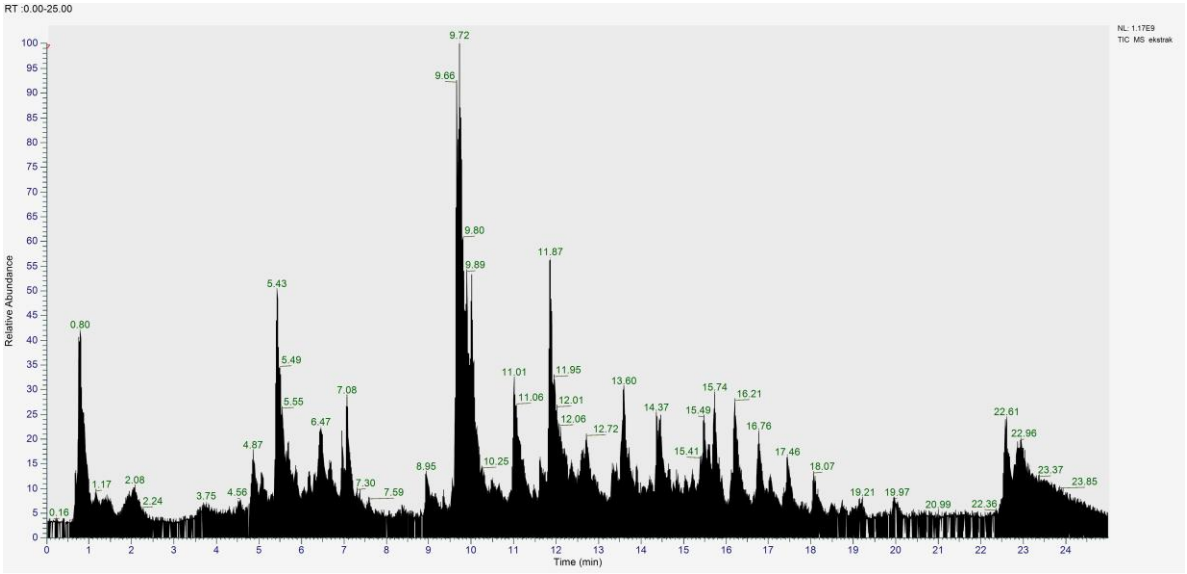

Figure 1. Total ion chromatogram (TIC) of the ethanolic extract of *Vitex trifolia* obtained by LC–HRMS in positive ESI mode. Peaks represent ion intensities detected across the chromatographic run.

Table 2. Major compounds detected in *Vitex trifolia* through LC–MS analysis

No	Compound	Molecular formula	Molecular weight (m/z)	Class	AUC (×10^6)
1	Casticin (NP-001928)	C19H18O8	374.099	Flavonoid	2384.32
2	(1ξ)-1,5-Anhydro-1-[2-(3,4-dihydroxyphenyl)-5,7-dihydroxy-4-oxo-4H-chromen-8-yl]-D-galactitol	C21H20O11	448.100	Flavonoid	773.48
3	(2S,3S,4S,5R,6S)-6-{[5,7-dihydroxy-2-(4-hydroxyphenyl)-4-oxo-4H-chromen-3-yl]oxy}-3,4,5-trihydroxyoxane-2-carboxylic acid	C21H18O12	462.079	Phenolic acid	522.29
4	5,7-dihydroxy-2-(3-hydroxy-4-methoxyphenyl)-3,6-dimethoxy-4H-chromen-4-one	C18H16O8	360.083	Flavonoid	455.82
5	4-Coumaric acid	C9H8O3	164.047	Phenolic acid	339.04
6	(1R,3R,4R,4aS)-4-Hydroxy-3,4a,8,8-tetramethyl-4-[2-(5-oxo-2,5-dihydro-3-furanyl)ethyl]decahydro-1-naphthalenyl acetate	C22H34O5	378.239	Diterpenoid	285.99

 doi:10.20944/preprints202511.1814.v1

7	(1r,3R,4s,5S)-4-{[(2E)-3-(3,4-dihydroxyphenyl)prop-2-enoyl]oxy}-1,3,5-trihydroxycyclohexane-1-carboxylic acid	C16H18O9	354.094	Phenolic acid	279.47
8	(1S,3R,4S,5R)-3,5-bis({[(2E)-3-(3,4-dihydroxyphenyl)prop-2-enoyl]oxy})-1,4-dihydroxycyclohexane-1-carboxylic acid	C25H24O12	516.126	Phenolic acid	273.62
9	Lupeol	C30H50O	426.385	Triterpenoid	229.73
10	4-Hydroxybenzoic acid	C7H6O3	138.032	Phenolic acid	161.62

2.2. Antioxidant and Enzymatic Bioactivities

To connect the chemical composition with its functional relevance, antioxidant assays (DPPH, ABTS, FRAP) were conducted and revealed robust radical-scavenging capacity (Table 3). The extract achieved IC_{50} values of 63.47 ± 0.24 µg/mL (DPPH) and 70.13 ± 1.28 µg/mL (ABTS), effectively neutralizing radicals via hydrogen atom transfer and single electron transfer mechanisms. FRAP analysis confirmed substantial reducing power (36.33 ± 0.18 $FeSO_4$ E/100 g extract). This multi-mechanistic antioxidant capacity aligns with the phenolic acids and methylated flavonoids identified by LC–HRMS, supporting *V. trifolia*'s cosmeceutical potential as a broad-spectrum antioxidant.

Table 3. Antioxidant activity of *Vitex trifolia* extract and ascorbic acid based on DPPH, ABTS and FRAP assay

Sample	IC_{50} – DPPH (µg/mL)	IC_{50} – ABTS (µg/mL)	FRAP assay ($FeSO_4$ E/100 g extract)
Ascorbic acid	5.39 ± 0.11	4.34 ± 0.08	316.04 ± 5.86
V. trifolia leaves extract	63.47 ± 0.24	70.13 ± 1.28	36.33 ± 0.18

Given that oxidative stress and enzymatic degradation are interconnected mechanisms in skin aging, the inhibitory activity of *V. trifolia* leaf extract against elastase and collagenase, two key enzymes involved in dermal ECM degradation, was further assessed (Table 4). *V. trifolia* extract displayed a moderate anti-elastase activity (IC_{50} = 400 ± 0.01 µg/mL) and a superior anti-collagenase activity (IC_{50} = 27.94 ± 3.20 µg/mL).

Table 4. Antielatase and anticollagenase activity of *Vitex trifolia* extract

Sample	IC_{50} – Antielastase (µg/mL)	IC_{50} – Anticollagenase (µg/mL)
Quercetin	5.50 ± 0.05	N/A
1,10-phenanthroline	N/A	3.27 ± 0.15
V. trifolia leaves extract	400 ± 0.01	27.94 ± 3.20

2.3. Cytoprotective Activity of Extract

The cell viability of HaCaT cells was plotted against different concentrations of standard and extracts shown in Figure 2. Cytotoxicity was evaluated according to ISO 10993-5, which considers a reduction in cell viability by more than 30% as indicative of cytotoxic potential [16]. Statistical analysis revealed that ascorbic acid significantly affected HaCaT cell viability starting at 50 µg/mL (Figure 2a), although cytotoxic potential was observed from 100 µg/mL. On the other hand, *V. trifolia* caused significant reductions in cell viability starting at 200 µg/mL, with cytotoxic effects appearing from 800 µg/mL (Figure 2b).

 doi:10.20944/preprints202511.1814.v1

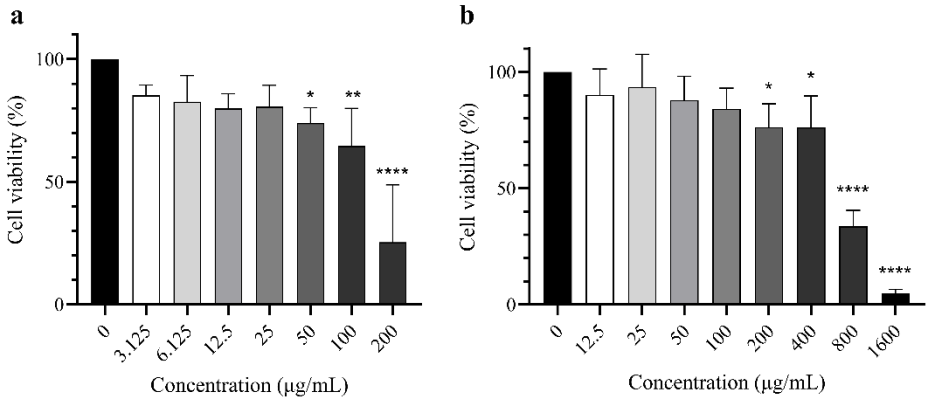

Figure 2. Cell viability (%) of HaCaT cells after treatment of different concentrations of (a) ascorbic acid and (b) *Vitex trifolia* after 24 hours treatment. Data are presented as mean ± SD (n=4). Statistical analysis (one-way ANOVA, Dunnett post-hoc) was done by comparing to negative controls of non-treated cells (0 µg/mL) *p<0.05; **p<0.01; ****p<0.0001; n = 4.

Data from cytotoxic assays were used as reference for the subsequent cytoprotective assays, in which only non-toxic concentrations of ascorbic acid and extracts were used for pre-treatment. The results of each treatment were shown in Figure 3. As positive control, ascorbic acid showed significant differences of protection in all concentrations (Figure 3a). Meanwhile, *V. trifolia* extracts showed a dose-dependent protective capability at concentrations from 12.5–200 µg/mL (Figure 3b). This indicates that the cytoprotective action of the extracts is effective within a certain concentration range. Therefore, 12.5 µg/mL was chosen as a treatment dose for the gene expression study, as it is the lowest concentration with cytoprotective effect and no cytotoxicity for all extracts.

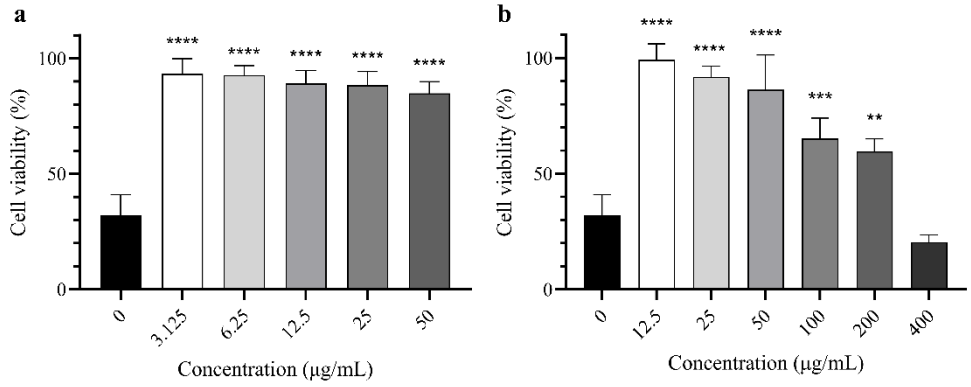

Figure 3. Cell viability (%) of HaCaT cells after 24 hours pre-treatment with (a) ascorbic acid and (b) *V. trifolia* and subsequent UVB exposure for 2 hours. Data are presented as mean ± SD (n=4). Statistical analysis (one-way ANOVA, Dunnett post-hoc) was done by comparing to negative controls of non-treated cells (0 µg/mL). NTC: cells not exposed to UVB. *p<0.05; **p<0.01; ***p<0.001; ****p<0.0001.

2.4. Analysis of MMP-1 and MMP-9 Expression

Expression of MMP-1 and MMP-9 gene was evaluated after treating the cells with extracts and then exposing the cells with UVB light source. UVB exposure was shown to significantly cause the upregulation of MMP-1 and MMP-9 expression in HaCaT cells (Figure 4). Interestingly, the result showed that treatment with *V. trifolia* reduced the MMP-9 by 51% though the MMP-1 remains unaffected. Following treatment and UVB-exposure, *V. trifolia* extract and ascorbic acid significantly reduced MMP-1 expression compared to non-treated controls by 42% and 27% respectively. Surprisingly, the extract showed significant reduction of MMP-9 expression compared to controls after UVB exposure by 69%.

 doi:10.20944/preprints202511.1814.v1

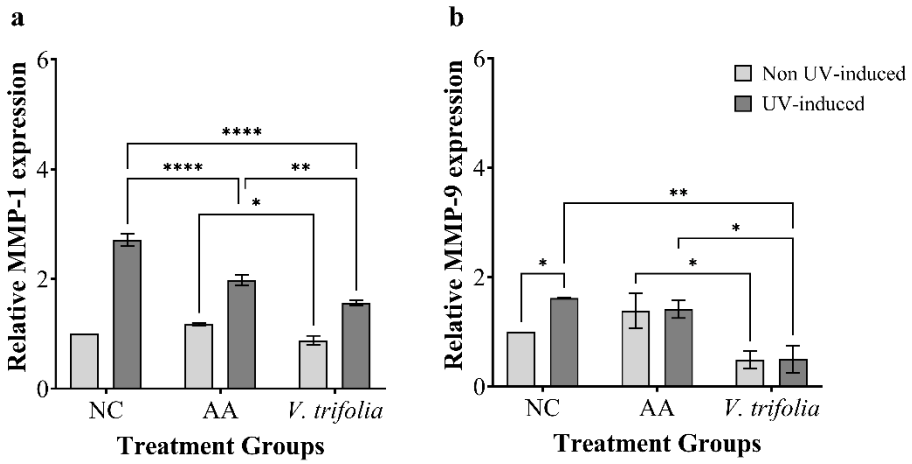

Figure 4. Relative gene expression of MMP-1 (a) and MMP-9 (b) in HaCaT cells after pre-treatment with *V. trifolia* extract and subsequent UVB exposure. Ascorbic acid (AA) served as a positive control and untreated cells (NC) as a negative control. Data are presented as mean ± SD (n=3). Statistical analysis (one-way ANOVA, Tukey's post-hoc test) was performed. **p<0.01; ****p<0.0001.

3. Discussion

Plants have long been explored as sources of bioactive compounds for cosmetic applications, largely because of their antioxidant, anti-aging, and skin-protective properties. These include plant extracts, fractions, and compounds [17,18]. However, before these natural products can be incorporated into formulations, their mechanisms of action and safety need to be carefully clarified [19,20]. Phenolic compounds, particularly flavonoids, are major contributors to antioxidant activity and modulation of ECM enzymes [21,22]. In addition to free radical scavenging, phenolics can modulate enzymes such as elastase and collagenase that are involved in ECM turnover, thereby contributing to anti-aging [23]. Furthermore, their antioxidant activity can provide photoprotective effects against UVB exposure [24].

In this study, the total phenolic content of *V. trifolia* extract was measured (78.52 ± 0.01 mg GAE/g extract), consistent to earlier reports where *V. trifolia* extracts generally contained less than 100 mg GAE/g [25]. Meanwhile, the total flavonoid content of the extract was reported as 1.99 ± 0.02 mg QE/g extract. Specialized flavonoids such as casticin and vitexin have been reported in *V. trifolia* at various values [12,26], and vitexicarpin has been isolated from *V. trifolia* in phytochemical studies [27]. The differences to variations likely arise from species-specific metabolism and environmental factors. Previous studies reported that altitude can modify phenolic content up to threefold, particularly in regions with high ultraviolet (UV) intensity [28,29]. This is because phenolic compounds function as protective molecules produced in response to environmental stress, including UV radiation [30]. Therefore, ecological and environmental conditions likely contributed to the phenolic differences observed between these species.

Building on this phytochemical foundation, our comprehensive LC–HRMS metabolomic analysis provides critical insights into the biochemical basis of *V. trifolia*'s skin-protective potential. The identification of the ten predominant high-abundance metabolites offers a molecular foundation for interpreting the extract's functional activities. The dominance of casticin and several structurally related flavonoids aligns closely with previous metabolomic reports on *Vitex* species [12,25,31], reflecting a phytochemical profile enriched in antioxidant and anti-inflammatory constituents. Casticin is particularly noteworthy, it has been widely documented for its potent ROS-scavenging capacity, its ability to attenuate UV-induced signaling pathways, and its inhibition of MMP activation [20,26,31], consistent with the antioxidant and anti-collagenase effects observed in our assays. Beyond flavonoids, the substantial presence of phenolic acids (e.g., 4-coumaric acid, 4-hydroxybenzoic acid, and conjugated phenolic derivatives) further reinforces the extract's redox-regulating effects, given their established hydrogen-donating, electron-transfer, and anti-protease properties [24,32,33].

 doi:10.20944/preprints202511.1814.v1

Additionally, the detection of terpenoids, including a diterpenoid derivative and lupeol, suggests complementary bioactivities, as terpenoids have been reported to support skin repair, enhance barrier function, and exert anti-inflammatory effects [34–36].

To contextualize these metabolomic findings, the antioxidant capacity of *V. trifolia* was evaluated using DPPH, ABTS, and FRAP assays, which together represent major antioxidant mechanisms involving single electron transfer (SET), hydrogen atom transfer (HAT), and ferric-reducing activity [37]. Phenolic compounds are key contributors to plant antioxidant behavior due to their radical-quenching, hydrogen-donating, and electron-transfer properties [33,38,39]. Consistent with this, *V. trifolia* exhibited strong radical-scavenging performance, with IC_{50} values of 63.47 ± 0.24 µg/mL (DPPH) and 70.13 ± 1.28 µg/mL (ABTS), indicating efficient neutralization of nitrogen- and carbon-centered radicals [37]. The extract also demonstrated meaningful reducing power in the FRAP assay (36.33 ± 0.18 $FeSO_4$ E/100 g extract).

Differences among the assays likely reflect solubility and physicochemical properties of the present antioxidants, as DPPH favors lipophilic molecules while ABTS accommodates a broader polarity range [39]. Even strong antioxidants such as ascorbic acid can show assay-dependent variability, displaying higher IC_{50} values across assays. Overall, the multi-mechanistic antioxidant activity observed corresponds closely with the LC–HRMS metabolite profile, particularly the abundance of methylated flavonoids, phenolic acids, and terpenoids, supporting a synergistic redox-balancing effect that may help mitigate oxidative stress, a key driver of photoaging and matrix degradation.

Building on this antioxidant potential, further assays were conducted to evaluate the extract's ability to inhibit key matrix-degrading enzymes involved in skin aging. Elastase, a serine endoprotease, specifically degrades elastin fibers maintaining skin elasticity. UV radiation-induced ROS upregulates elastase expression up to fourfold, promoting elastosis through abnormal elastin accumulation [40]. Meanwhile, collagenase (MMP-1), a zinc-dependent metalloproteinase, degrades type I and III dermal collagen, leading to wrinkle formation following UV exposure and oxidative stress [41].

The *V. trifolia* extract exhibited a moderate anti-elastase effect (IC_{50} = 400 ± 0.01 µg/mL) and a notably strong anti-collagenase activity (IC_{50} = 27.94 ± 3.20 µg/mL). The superior collagenase inhibition is consistent with the extract's abundance of flavonoids, particularly casticin and related derivatives, which have been reported to chelate Zn^{2+} at the MMP catalytic site and suppress MMP-1 activity [32,42]. The observed IC_{50} value falls within the range of established natural inhibitors such as *Centella asiatica* (45.3 µg/mL) and *Camellia sinensis* polyphenols (~30 µg/mL) [41,43], highlighting the potential of *V. trifolia* as a promising anti-collagenase agent for preventing UV-induced dermal collagen degradation in cosmetic applications.

Following the enzymatic inhibition results, the cellular safety of *V. trifolia* extracts was evaluated in HaCaT cells, a human keratinocyte model for epidermal studies, thus a model for topical formulations [44]. Cytotoxicity was assessed by measuring cell viability at different extract concentrations using the one-step 3-(4,5-Dimethylthiazol-2-yl)-5-(3-carboxymethoxyphenyl)-2-(4-sulfophenyl)-2H-tetrazolium (MTS) assay, a colorimetric method in which metabolically active cells reduce tetrazolium to a soluble formazan dye (Riss et al., 2016; Boyraz et al., 2021). Based on ISO 10993-5 criteria, extracts that reduce cell viability by more than 30% indicate cytotoxic potential [16]. Ascorbic acid, the positive control, expressed cytotoxic effects starting from concentration as low as 100 µg/mL. This cytotoxicity is attributed to ascorbic acid's ability to generate extracellular hydrogen peroxide, particularly in the presence of metal ions, leading to oxidative stress and cell death [45–47]. The extent of toxicity depends on the cells' capacity to detoxify hydrogen peroxide, primarily via catalase, with cells expressing lower catalase levels (such as HaCaT), being more susceptible [46]. *V. trifolia* exhibited a relatively wide safety margin, remaining non-toxic at concentrations as high as 800 µg/mL, unlike that of ascorbic acid. These results are consistent with previous safety data in other cell lines [48,49].

 doi:10.20944/preprints202511.1814.v1

Subsequently, cytoprotective assay was performed to determine whether the extracts could mitigate UVB-induced oxidative damage in keratinocytes, evaluating a compound's ability to preserve cell viability and integrity under stress conditions such as UV exposure or chemical insult [50]. In this study, the cell was treated with extracts and exposed with UVB light with a 2.484 J/cm^2 dose for 2 hours after 24 hours of treatment, a dose under the range commonly used to model 40 min of midday sun exposure with a UV index of 6 [51]. Cytotoxic effects that exhibited from UVB irradiation to HaCaT cells were likely caused by increases in intracellular ROS levels resulting in oxidative stress that damages components of cells such proteins, DNA, and lipids [52]. This oxidative damage reduces the viability and functionality of cells. Moreover, UVB radiation promotes the production of ROS including hydrogen peroxide (H_2O_2), hydroxyl radicals (-OH), and superoxide anion radicals (O_2^-) [53]. These ROS are produced by UVB-induced photochemical reactions and cellular metabolic activities.

Both extract and ascorbic acid demonstrated cytoprotective effects within specific concentration ranges. Ascorbic acid exhibited protection at concentration range as low as 3.125–25 µg/mL, consistent with its known antioxidant activity at low doses [54,55]. However, at ≥50 µg/mL, it became pro-oxidant, producing hydrogen peroxide and ROS that induced apoptosis and reduced cell viability [54]. Meanwhile, *V. trifolia* extract exhibited protection starting at concentration 12.5 µg/mL. The activity of plant extracts is dose-dependent, with higher concentrations potentially triggering apoptosis or cell cycle arrest due to combined effects of multiple bioactive compounds [56]. In contrast, *V. trifolia* extract displayed a broader protective range (12.5–50 µg/mL), consistent with reports of its ability to reduce ROS and modulate inflammatory signaling pathways [36]. The extract's cytoprotective function is enhanced by its capacity to control inflammatory cytokines and signalling pathways, which enables it to sustain cell viability over a wider concentration range than extracts with fewer effective dosages.

As previously discussed, UVB exposure rapidly generates ROS in keratinocytes, resulting in oxidative stress that is a central trigger for skin damage and photoaging [57]. ROS is capable of activating key intracellular signaling pathways, primarily the mitogen-activated protein kinase (MAPK) cascade (which includes ERK, JNK, and p38 [58,59]. By activating the MAPKs, the transcription factor complex activator protein 1 (AP-1) which are the primary regulator of MMPs gene transcription, was then phosphorylated and activated [60]. AP-1 is then bound to TPA-responsive elements in the promoter region of MMP-1 and MMP-9 genes, hence upregulating their expression [59].

Our results suggested that flavonoids and phenolic compounds in the extracts may act as ROS scavengers, thereby reducing the oxidative stress triggered by UVB exposure and subsequently suppressing NF-κB/MAPK pathway activation that drives MMP gene expression. Such mechanisms align with previous findings showing that flavonoid-rich extracts inhibit UVB-induced MAPK activation and downstream MMP upregulation [58]. Consistent with this, UVB irradiation markedly elevated MMP-1 and MMP-9 expression in HaCaT cells, as expected from UVB-induced ROS stimulation of AP-1-mediated transcription [60]. Treatment with *V. trifolia* extract demonstrated a notable modulatory effect, in which under non-UVB conditions, it reduced basal MMP-1 expression by 42% and MMP-9 by 69%, suggesting intrinsic anti-inflammatory or matrix-regulating activity, which is consistent with reports of *V. trifolia* flavonoids suppressing pro-inflammatory gene expression [31]. In contrast, ascorbic acid showed only moderate suppression of MMP-1, likely due to its limited stability and tendency to act as a pro-oxidant behavior under oxidative stress [61]. Because UVB-driven ROS strongly induces both MMP-1 and MMP-9, the substantial inhibition observed indicates that *V. trifolia* effectively attenuates upstream oxidative and inflammatory cascades, with its particularly strong suppression of MMP-9 highlighting its potential as a potent anti-photoaging agent [6].

Overall, the findings of this study demonstrate that *V. trifolia* possesses a multifaceted skin-protective potential, combining strong antioxidant activity, selective enzyme inhibition, cytoprotective effects and suppression of UVB-induced MMP expression. Its rich flavonoid and

 doi:10.20944/preprints202511.1814.v1

phenolic content underlie both its ROS-scavenging capacity and its modulation of inflammatory and matrix-degrading pathways, suggesting a dual role in preventing oxidative damage and mitigating ECM breakdown. The broad safety margin observed in HaCaT cells further supports its suitability for topical application. Collectively, these results highlight *V. trifolia* as a promising natural ingredient for anti-photoaging cosmetic formulations, capable of protecting skin from UV-induced oxidative stress while regulating key enzymes and pathways implicated in wrinkle formation and tissue degradation. Future studies exploring formulation stability, bioavailability, and *in vivo* efficacy will be essential to fully realize its cosmeceutical potential.

4. Materials and Methods

4.1. Extract Preparation

Leaves of *Vitex trifolia* were collected from Bogor, West Java, Indonesia and taxonomically identified by Biopharmaca Research Center, Bogor, Indonesia (voucher specimen number BMK0171092016). The leaves were cleaned, dried in a drying cabinet at 30–40 °C for 5 days, ground into powder, and sieved. *V. trifolia* was extracted using MAE with 96% ethanol at a 1:10 (w/v) ratio of leaf powder to solvent. The extraction was performed at low microwave power (30%) for 10 min and repeated three times, followed by filtration. The combined filtrates were concentrated using a rotary evaporator and further thickened in a water bath until a constant mass was obtained.

4.2. Determination of Total Phenolic Content (TPC)

The Folin-Ciocalteu (FC) method was used to examine TPC of extract. Gallic acid (GAE) was used as a standard for calibration (5 to 50 µg/mL concentration). In a 96-well plate, 15 µL each of standard or sample was mixed with 75 µL of 10% (v/v) FC Reagent (Merck). After 8 minutes, 75 µL of 7.5% sodium bicarbonate was added. The plate was incubated for one hour at room temperature, and the absorbance was measured at 765 nm. The experiment was done in triplicate. Results were expressed as mg gallic acid equivalent (GAE)/g extract.

4.3. Determination of Total Flavonoid Content (TFC)

TFC was measured using the aluminum chloride colorimetric method. Quercetin was used as standard for calibration (5 to 50 µg/mL concentration). In a 96-well plate, 20 µL of each standard or sample was mixed with 80 µL methanol. Subsequently, 6 µL of 5% sodium nitrate was added, followed by 6 µL of 10% aluminum chloride after 3 minutes. After an additional 3 minutes, 40 µL of 1 M sodium hydroxide was added. The experiment was performed in triplicate, and the absorbance was measured at 510 nm. TFC was expressed as mg quercetin equivalent (QE)/g extract.

4.4. Metabolomic Profiling by Liquid Chromatography High Resolution Mass Spectrometry (LC–HRMS)

LC–HRMS analysis was performed using a Vanquish™ UHPLC system coupled to a Q Exactive™ Hybrid Quadrupole-Orbitrap™ mass spectrometer (Thermo Scientific, Germany) equipped with electrospray ionization (ESI) in positive mode. Chromatographic separation was achieved on an Accucore™ Phenyl-Hexyl column (100 × 2.1 mm, 2.6 µm) using a mobile phase consisting of water + 0.1% formic acid (A) and acetonitrile + 0.1% formic acid (B) at 0.3 mL·min^{-1}. The gradient program increased from 5% to 90% B over 16 minutes, followed by a 4-minute isocratic hold at 90% B, then re-equilibration to initial conditions (total run time: 25 minutes). Samples (5–10 mg) were dissolved in MS-grade solvent, ultrasonicated for 30 minutes, and filtered through 0.22 µm PTFE membranes before injection (3 µL). Full MS/data-dependent MS^2 (dd-MS^2) spectra were acquired over m/z 66.7–1000 with resolving powers of 70,000 (full MS) and 17,500 (MS^2), using the following parameters: spray voltage 3.30 kV, capillary temperature 320°C, and sheath/auxiliary/sweep gas flows at 32/8/4 AU, respectively. Data processing was performed using

 doi:10.20944/preprints202511.1814.v1

Compound Discoverer™ 3.2 software, with compound annotation based on spectral matching against mzCloud™ and ChemSpider™ databases using a ±5 ppm mass accuracy threshold.

4.5. Antioxidant Assays

4.5.1. 2,2-Diphenyl-1-Picrylhydrazyl (DPPH) Assay

DPPH assay was done according to Lee et al., (2015) with minor modifications. The DPPH reagent was made at a concentration of 0.1 mM. Extract samples were diluted into a series of concentrations (12.5 up to 800 µg/mL). Ascorbic acid was used as positive control (3.125 to 100 µg/mL). In a 96-well plate, equal volumes of each extract or standard solution and the DPPH solution were mixed. Methanol was used as the solvent blank. The plate was incubated in the dark at room temperature for 30 minutes. Following incubation, absorbance was measured at 517 nm. The percentage of DPPH radical scavenging activity was calculated using the formula:

4.5.2. 2,2'-Azino-Bis(3-Ethylbenzothiazoline-6-Sulfonic Acid) (ABTS) Assay

Antioxidant activity test with ABTS method was done by following Lee et al, (2015) with minor modifications. ABTS as a radical was made by mixing 5 mL of 7 mM ABTS with 88 µL of 140 mM $K_2S_2O_8$ solution, followed by incubation for 16 hours in the dark and dilution with distilled water at a ratio of 1:15. Ascorbic acid was used as standard (1 to 13 µg/mL concentration). Plant extracts were diluted in methanol. In a 96-well plate, 100 µL of extract or standard and 100 µL of diluted ABTS reagent was added, then incubated in the dark at room temperature for 6 minutes. The absorbance was measured at 745 nm. Using the linear curve obtained from equation (1), IC_{50} was calculated with equation (2):

$$IC50\ (\mu g/mL) = \frac{50-c}{Absorbance\ blank} \times 100\% \quad (2)$$

where c stands for constant and m stands for slope in a linear equation (y=mx+c).

4.5.3. Ferric Reducing Antioxidant Power (FRAP) Assay

Antioxidant activity test with FRAP method was done by following Bolaños de la Torre *et al.* (2015) with minor modification. The FRAP reagent was prepared by mixing 25 mL of 300 mM acetate buffer, 2.5 mL of 20 mM $FeCl_3 \cdot 6H_2O$, and 2.5 mL of 10 mM TPTZ in 40 mM HCl (10:1:1, v/v/v). $FeSO_4 \cdot 7H_2O$ was used as standard (75 to 200 µM concentration), while ascorbic acid (10 µg/mL) was used as the positive control. In a 96-well plate, 50 µL of plant extract or standard solution was mixed with 150 µL of FRAP reagent and incubated at 37 °C for 30 minutes in the dark. Absorbance was measured at 597 nm using a microplate reader. The FRAP value was determined with equation (3):

$$FRAP\ value\ (\mu mol\ Fe^{2+}/g\ sample) = \frac{x}{K} \quad (3)$$

where x is concentration equivalent from the calibration curve $FeSO_4 \cdot 7H_2O$ (µM) and K is sample concentration (g/L).

Antioxidant activity was then expressed as $FeSO_4 \cdot 7H_2O$ equivalents (g/100 g sample) calculated as equation (4):

$$AA(FeSO4.7H2O\ Eq) = \frac{FRAP \times Mr \times 100\ g\ sample}{10^6 \mu mol} \quad (4)$$

4.6. Antielastase Assay

Elastase inhibition was evaluated following Anggraini (2020) and Suwandy (2023), with modifications. Extracts were dissolved in the Tris-HCl buffer (100 mM, pH 8). Quercetin was used as positive control. In a 96-well plate, sample solutions were mixed with Tris-HCl buffer and 20 µL of elastase (0.22 U/mL), followed by incubation at 25 °C for 15 min. Subsequently, 30 µL of 1.3 mM N-succinyl-(Ala)3-p-nitroanilide (SANA) substrate was added, and the mixture was incubated for 30

 doi:10.20944/preprints202511.1814.v1

min at room temperature. Absorbance was measured at 405 nm using a microplate reader. Antielastase activity was calculated based on equation (5):

$$Antielastase\ activity\ (\%) = \frac{[(ABE-AB)-(ASE-AS)]}{(ABE-AB)} \times 100\% \quad (5)$$

where ABE is absorbance of blank with enzyme, AB is absorbance of blank without enzyme, ASE is absorbance of extract or control with enzyme, and AS is absorbance of extract or control without enzyme.

Subsequently, the concentration of sample needed to inhibit 50% enzyme (IC_{50}) was calculated based on the calibration curve calculated using equation (2).

4.7. Anticollagenase Assay

Anticollagenase activity was determined according to the method of Wittenauer et al., 2015 with modifications. The anti-collagenase activity of *V. trifolia* leaf extract was evaluated against the standard inhibitor 1,10-phenanthroline using a microplate reader based on the hydrolysis of the synthetic substrate FALGPA by *Clostridium histolyticum* collagenase (ChC). Each extract solution is first diluted with 2 µL 2% DMSO. The reaction mixture consisted of 35 µL of ChC solution (1.65 U/mL), extracts/standard sample solution, and Tris-HCl buffer (100 mM, pH 7.5) to a final volume of 200 µL. This mixture was incubated at 37°C for 20 min. The reaction was initiated by adding 33 µL of 0.33 mM FALGPA solution. The final concentration ranges were 1-5 µg/mL for 1,10-phenanthroline and 10-50 µg/mL for *V. trifolia* leaf extract. The decrease in absorbance of FALGPA was monitored at 345 nm for 15 min using a microplate reader (Sigma-Aldrich). Substrate-free blanks and enzyme-free controls were included. Sample and blank readings were corrected using the enzyme-free controls. All assays were performed in triplicate. The inhibitory effect of the sample on anti-collagenase activity was calculated using the same equation as equation (5). Subsequently, the concentration of sample needed to inhibit 50% enzyme (IC_{50}) was calculated based on the calibration curve calculated using equation (2).

4.8. Cell Culture

Immortalized human keratinocytes (HaCaT) were maintained in Dulbecco's Modified Eagle Medium (DMEM, Gibco, USA), 10% fetal bovine serum (FBS, Gibco, USA) and 1% penicillin-streptomycin (Gibco, USA). Cells were cultured in a humidified incubator at 37°C with 5% CO_2 atmosphere. Upon reaching 80-90% confluency, cells were harvested with 0.25% trypsin-EDTA (Gibco, USA).

4.9. Cytotoxicity Assay

The cytotoxic effects of *Vitex trifolia* extract as samples and ascorbic acid as a positive control were evaluated under ISO 10993-5 criteria using the MTS assay (Promega, USA), also known as one-step 3-(4,5-dimethylthiazol-2-yl)-2,5-diphenyltetrazolium bromide (MTT) assay. HaCaT cells were seeded into 96-well plates at a density of 1 x 10^4 cells/well and incubated under standard culture conditions (37°C, 5% CO2). After 24 hours and reaching 80-90% confluency, the culture medium was replaced with fresh media containing the test compounds at varying concentrations (12.5 - 1600 µg/mL). Following a 24-hour incubation, the treatment media were removed and replaced with fresh media. A volume of 20 µL of MTS reagent was added to each well. The plates were incubated for 3 hours in the dark (37°C, 5% CO_2) and absorbance was measured at 490 nm using a microplate reader (TECAN, Switzerland). Cell viability (%) was calculated by comparing the absorbance of cells treated with extracts to those without treatment.

4.10. Cytoprotective Assay Against UVB-Induced Damage

HaCaT cells were seeded and cultured as described in Section 4.7. Upon reaching 80–90% confluency, the cells were pretreated for 24 hours with non-cytotoxic concentrations of *V. trifolia*

 doi:10.20944/preprints202511.1814.v1

extract, or ascorbic acid (concentrations determined from Section 4.8). After pre-treatment, the medium was removed, and the cells were washed once with phosphate buffered saline (PBS). Cells were then subjected to UVB irradiation inside a UV box at a distance of 10 cm from the light source at a dose of 2.484 J/cm2 over a 2-hour exposure period. Wells containing untreated (media-only) cells and wells protected from UVB using aluminum foil served as controls. Immediately following UVB exposure, the medium was replaced with fresh media containing MTS reagent (5:1 ratio), and the plate was incubated in the dark for 3 hours (37°C, 5% CO_2). Absorbance measurement and cell viability calculation followed the exact procedure detailed in Section 4.8.

4.11. Gene Expression Analysis of MMP-1 and MMP-9 Using Quantitative Real-Time Polymerase Chain Reaction (qRT-PCR)

HaCaT cells were seeded, pretreated with non-cytotoxic concentrations of the extracts/ascorbic acid for 24 hours, and then subjected to UVB irradiation (2.484 J/cm2 for 2 hours) exactly as described in Section 4.9. Following the 2-hour UVB exposure, the cells were incubated for 24 hours before being harvested for RNA isolation. Total RNA was extracted from the cells using the Total RNA mini kit (Geneaid, Taiwan) according to the manufacturer's protocol. RNA concentration and purity were determined using NanoDrop Lite Plus Spectrophotometer (Thermo Fisher Scientific, USA) with A260/A280 ratio criteria. Gene expression was analyzed by synthesizing cDNA from the RNA template using ReverTra Ace™ qPCR RT Master Mix (Toyobo, Japan). Synthesized cDNA underwent PCR amplification using SensiFAST SYBR No-ROX Kit (Meridian Bioscience, USA) and primers. Target genes included MMP-1 and MMP-9. The reference gene used for normalization was GAPDH. Primer sequences for all genes were obtained and purchased from (Macrogen, South Korea). The primer sequences were: GAPDH (forward 5′-AAGCCTGCCGGTGACTAACT-3′, reverse 5′-TCGCTCCACCTGACTTCC-3′), MMP-1 (forward 5′-CATGCTTTTCAACCAGGCCC-3′, reverse 5′-GGTACATCAAAGCCCCGAT-3′), and MMP-9 (forward 5′-TTTGACAGCGACAAGAAGT-3′, reverse 5′-CATTCACGTCCTTATGC-3′). RT-qPCR was performed on RT-PCR Rotor Gene Q (Qiagen, Canada) using the thermal cycling conditions recorded in Table 5. Relative gene expression was calculated using the comparative Ct method ($2^{-\Delta\Delta Ct}$).

Table 5. Thermal profile used for qRT-PCR amplification

Step	Cycle	Temperature (°C)	Duration
Initial denaturation	1	95	2 min
Denaturation		95	5 s
Annealing	40	65	10 s
Extension		72	20 s

4.12. Data and Statistical Analysis

The data obtained from the experiment were analyzed and processed with GraphPad Prism 10. Normality was assessed using the Shapiro-Wilk test. Data that were normally distributed were statistically analyzed using one-way analysis of variance (ANOVA). Dunnett's post hoc test was done to compare multiple treatment groups to a single control group, specifically on cytotoxic and cytoprotective assays. Meanwhile, Tukey's post hoc test was done to compare all possible pairs of means, specifically on gene expression studies. The significance level of $p<0.05$ was considered statistically significant.

5. Conclusions

Vitex trifolia ethanolic leaf extract demonstrates substantial cosmeceutical potential through a combination of antioxidant, enzymatic, and photoprotective activities. Its flavonoid- and phenolic-rich composition effectively scavenges UVB-induced ROS, attenuating MAPK/NF-κB signaling and leading to significant downregulation of MMP-1 and MMP-9 expression. The extract exhibits

 doi:10.20944/preprints202511.1814.v1

stronger collagenase inhibition relative to elastase, is non-cytotoxic up to 100 μg/mL, and provides cytoprotection in HaCaT cells at 12.5–50 μg/mL. These multi-targeted actions suggest that *V. trifolia* is a promising natural ingredient for preventing extracellular matrix degradation and photoaging, supporting its safe and effective use in skin-protective cosmeceutical formulations.

Author Contributions: Conceptualization, D.M.A., P.H.; methodology D.M.A., P.H., A.M., C.C.Y.; software, C.C., M.L.W., R.F., E.C.; validation, D.M.A., P.H., R.F.; formal analysis, D.M.A., P.H., C.C., F.K.T.W., N.D.L., M.L.W., E.C.; investigation, D.M.A., P.H., C.C., F.K.T.W., N.D.L., M.L.W.; resources, D.M.A., P.H., A.M.; data curation, D.M.A., C.C., F.K.T.W., N.D.L., M.L.W., P.G.M.W.M., E.C.; writing—original draft preparation, D.M.A., P.H., R.F., E.C; writing—review and editing, D.M.A., P.H., R.F., R.J.J., S.M., E.C.; visualization, D.M.A., C.C., F.K.T.W., M.L.W., R.F., P.G.M.W.M., E.C.; supervision, D.M.A., P.H.; project administration, R.F., E.C.; funding acquisition, D.M.A., R.J.J., S.M., C.C.Y. All authors have read and agreed to the published version of the manuscript.

Funding: This research was funded by Universitas Indonesia through PUTI, grant number NKB-174/UN2.RST/HKP.05.00/2024.

Data Availability Statement: The data presented in this study is available on request from the corresponding author.

Acknowledgments: The authors gratefully acknowledge PUTI for the funding of this article.

Conflicts of Interest: The authors declare no conflicts of interest.

Abbreviations

ABTS	2,2′-azino-bis(3-ethylbenzothiazoline-6-sulfonic acid)
AP-1	Activator protein-1
DPPH	2,2-diphenyl-1-picrylhydrazyl
ECM	Extracellular matrix
FRAP	Ferric reducing antioxidant power
GAE	Gallic acid equivalent
HAT	Hydrogen atom transfer
LC–HRMS	Liquid chromatography–high resolution mass spectrometry
MAE	Microwave-assisted extraction
MAPK	Mitogen-activated protein kinase
MMP	Matrix metalloproteinase
MTT	3-(4,5-dimethylthiazol-2-yl)-2,5-diphenyltetrazolium bromide
MTS	3-(4,5-dimethylthiazol-2-yl)-5-(3-carboxymethoxyphenyl)-2-(4-sulfophenyl)-2H-tetrazolium
PBS	Phosphate-buffered saline
QE	Quercetin equivalent
qRT-PCR	Quantitative real-time polymerase chain reaction
ROS	Reactive oxygen species
SANA	N-succinyl-(Ala)3-p-nitroanilide
SET	Single electron transfer
TFC	Total flavonoid content
TPC	Total phenolic content
UVB	Ultraviolet B

References

1. Tomas, M.; Günal-Köroğlu, D.; Kamiloglu, S.; Ozdal, T.; Capanoglu, E. The State of the Art in Anti-Aging: Plant-Based Phytochemicals for Skin Care. *Immunity & Ageing* **2025**, *22*, 5, doi:10.1186/s12979-025-00498-9.
2. Zhang, J.; Yu, H.; Man, M.; Hu, L. Aging in the Dermis: Fibroblast Senescence and Its Significance. *Aging Cell* **2024**, *23*, doi:10.1111/acel.14054.
3. Wei, M.; He, X.; Liu, N.; Deng, H. Role of Reactive Oxygen Species in Ultraviolet-Induced Photodamage of the Skin. *Cell Div* **2024**, *19*, 1, doi:10.1186/s13008-024-00107-z.

 doi:10.20944/preprints202511.1814.v1

4. Kim, S.R.; Park, J.W.; Lee, B.-H.; Lim, K.M.; Chang, T.-S. Peroxiredoxin V Protects against UVB-Induced Damage of Keratinocytes. *Antioxidants* **2023**, *12*, 1435, doi:10.3390/antiox12071435.
5. Salminen, A.; Kaarniranta, K.; Kauppinen, A. Photoaging: UV Radiation-Induced CGAS-STING Signaling Promotes the Aging Process in Skin by Remodeling the Immune Network. *Biogerontology* **2025**, *26*, 123, doi:10.1007/s10522-025-10268-1.
6. Kim, D.J.; Iwasaki, A.; Chien, A.L.; Kang, S. UVB-Mediated DNA Damage Induces Matrix Metalloproteinases to Promote Photoaging in an AhR- and SP1-Dependent Manner. *JCI Insight* **2022**, *7*, doi:10.1172/jci.insight.156344.
7. Hu, X.; Chen, M.; Nawaz, J.; Duan, X. Regulatory Mechanisms of Natural Active Ingredients and Compounds on Keratinocytes and Fibroblasts in Mitigating Skin Photoaging. *Clin Cosmet Investig Dermatol* **2024**, *Volume 17*, 1943–1962, doi:10.2147/CCID.S478666.
8. Pittayapruek, P.; Meephansan, J.; Prapapan, O.; Komine, M.; Ohtsuki, M. Role of Matrix Metalloproteinases in Photoaging and Photocarcinogenesis. *Int J Mol Sci* **2016**, *17*, 868, doi:10.3390/ijms17060868.
9. Geng, R.; Kang, S.-G.; Huang, K.; Tong, T. Boosting the Photoaged Skin: The Potential Role of Dietary Components. *Nutrients* **2021**, *13*, 1691, doi:10.3390/nu13051691.
10. Dwevedi, D.; Srivastava, A. Molecular Mechanisms of Polyphenols in Management of Skin Aging. *Curr Aging Sci* **2024**, *17*, 180–188, doi:10.2174/0118746098287130240212085507.
11. Kamal, N.; Mio Asni, N.S.; Rozlan, I.N.A.; Mohd Azmi, M.A.H.; Mazlan, N.W.; Mediani, A.; Baharum, S.N.; Latip, J.; Assaw, S.; Edrada-Ebel, R.A. Traditional Medicinal Uses, Phytochemistry, Biological Properties, and Health Applications of *Vitex* Sp. *Plants* **2022**, *11*, 1944, doi:10.3390/plants11151944.
12. Mottaghipisheh, J.; Kamali, M.; Doustimotlagh, A.H.; Nowroozzadeh, M.H.; Rasekh, F.; Hashempur, M.H.; Iraji, A. A Comprehensive Review of Ethnomedicinal Approaches, Phytochemical Analysis, and Pharmacological Potential of *Vitex Trifolia* L. *Front Pharmacol* **2024**, *15*, doi:10.3389/fphar.2024.1322083.
13. Cavinato, M.; Waltenberger, B.; Baraldo, G.; Grade, C.V.C.; Stuppner, H.; Jansen-Dürr, P. Plant Extracts and Natural Compounds Used against UVB-Induced Photoaging. *Biogerontology* **2017**, *18*, 499–516, doi:10.1007/s10522-017-9715-7.
14. Chaikhong, K.; Chumpolphant, S.; Rangsinth, P.; Sillapachaiyaporn, C.; Chuchawankul, S.; Tencomnao, T.; Prasansuklab, A. Antioxidant and Anti-Skin Aging Potential of Selected Thai Plants: *In Vitro* Evaluation and In Silico Target Prediction. *Plants* **2022**, *12*, 65, doi:10.3390/plants12010065.
15. Olivero-Verbel, J.; Quintero-Rincón, P.; Caballero-Gallardo, K. Aromatic Plants as Cosmeceuticals: Benefits and Applications for Skin Health. *Planta* **2024**, *260*, 132, doi:10.1007/s00425-024-04550-8.
16. *ISO 10993-5:2009 Biological Evaluation of Medical Devices — Part 5: Tests for in Vitro Cytotoxicity*; Geneva, 2009;
17. Ribeiro, A.; Estanqueiro, M.; Oliveira, M.; Sousa Lobo, J. Main Benefits and Applicability of Plant Extracts in Skin Care Products. *Cosmetics* **2015**, *2*, 48–65, doi:10.3390/cosmetics2020048.
18. Lee, J.; Hyun, C.-G. Natural Products for Cosmetic Applications. *Molecules* **2023**, *28*, 534, doi:10.3390/molecules28020534.
19. Resende, D.I.S.P.; Jesus, A.; Sousa Lobo, J.M.; Sousa, E.; Cruz, M.T.; Cidade, H.; Almeida, I.F. Up-to-Date Overview of the Use of Natural Ingredients in Sunscreens. *Pharmaceuticals* **2022**, *15*, 372, doi:10.3390/ph15030372.
20. Luo, J.; Si, H.; Jia, Z.; Liu, D. Dietary Anti-Aging Polyphenols and Potential Mechanisms. *Antioxidants* **2021**, *10*, 283, doi:10.3390/antiox10020283.
21. de Lima Cherubim, D.J.; Buzanello Martins, C.V.; Oliveira Fariña, L.; da Silva de Lucca, R.A. Polyphenols as Natural Antioxidants in Cosmetics Applications. *J Cosmet Dermatol* **2020**, *19*, 33–37, doi:10.1111/jocd.13093.
22. Crespi, O.; Rosset, F.; Pala, V.; Sarda, C.; Accorinti, M.; Quaglino, P.; Ribero, S. Cosmeceuticals for Anti-Aging: Mechanisms, Clinical Evidence, and Regulatory Insights—A Comprehensive Review. *Cosmetics* **2025**, *12*, 209, doi:10.3390/cosmetics12050209.
23. Wittenauer, J.; Mäckle, S.; Sußmann, D.; Schweiggert-Weisz, U.; Carle, R. Inhibitory Effects of Polyphenols from Grape Pomace Extract on Collagenase and Elastase Activity. *Fitoterapia* **2015**, *101*, 179–187, doi:10.1016/j.fitote.2015.01.005.

 doi:10.20944/preprints202511.1814.v1

24. Rudrapal, M.; Khairnar, S.J.; Khan, J.; Dukhyil, A. Bin; Ansari, M.A.; Alomary, M.N.; Alshabrmi, F.M.; Palai, S.; Deb, P.K.; Devi, R. Dietary Polyphenols and Their Role in Oxidative Stress-Induced Human Diseases: Insights Into Protective Effects, Antioxidant Potentials and Mechanism(s) of Action. *Front Pharmacol* **2022**, *13*, doi:10.3389/fphar.2022.806470.
25. Saklani, S.; Mishra, A.; Chandra, H.; Atanassova, M.; Stankovic, M.; Sati, B.; Shariati, M.; Nigam, M.; Khan, M.; Plygun, S.; et al. Comparative Evaluation of Polyphenol Contents and Antioxidant Activities between Ethanol Extracts of Vitex Negundo and Vitex Trifolia L. Leaves by Different Methods. *Plants* **2017**, *6*, 45, doi:10.3390/plants6040045.
26. Chan, E.W.C.; Wong, S.K.; Chan, H.T. Casticin from Vitex Species: A Short Review on Its Anticancer and Anti-Inflammatory Properties. *J Integr Med* **2018**, *16*, 147–152, doi:10.1016/j.joim.2018.03.001.
27. Wang, H.; Cai, B.; Cui, C.; Zhang, D.; Yang, B. Vitexicarpin, a Flavonoid from *Vitex Trifolia* L., Induces Apoptosis in K562 Cells via Mitochondria-Controlled Apoptotic Pathway. *Yao Xue Xue Bao* **2005**, *40*, 27–31.
28. Jaakola, L.; Hohtola, A. Effect of Latitude on Flavonoid Biosynthesis in Plants. *Plant Cell Environ* **2010**, *33*, 1239–1247, doi:10.1111/j.1365-3040.2010.02154.x.
29. Gülsoy, E.; Kaya, E.D.; Türkhan, A.; Bulut, M.; Koyuncu, M.; Güler, E.; Sayın, F.; Muradoğlu, F. The Effect of Altitude on Phenolic, Antioxidant and Fatty Acid Compositions of Some Turkish Hazelnut (Coryllus Avellana L.) Cultivars. *Molecules* **2023**, *28*, 5067, doi:10.3390/molecules28135067.
30. Zoratti, L.; Karppinen, K.; Luengo Escobar, A.; HÃ¤ggman, H.; Jaakola, L. Light-Controlled Flavonoid Biosynthesis in Fruits. *Front Plant Sci* **2014**, *5*, doi:10.3389/fpls.2014.00534.
31. Annamalai, P.; Thangam, E.B. *Vitex Trifolia* L. Modulates Inflammatory Mediators via down-Regulation of the NF-KB Signaling Pathway in Carrageenan-Induced Acute Inflammation in Experimental Rats. *J Ethnopharmacol* **2022**, *298*, 115583, doi:10.1016/j.jep.2022.115583.
32. Thring, T.S.; Hili, P.; Naughton, D.P. Anti-Collagenase, Anti-Elastase and Anti-Oxidant Activities of Extracts from 21 Plants. *BMC Complement Altern Med* **2009**, *9*, 27, doi:10.1186/1472-6882-9-27.
33. Sánchez-Rangel, J.C.; Benavides, J.; Heredia, J.B.; Cisneros-Zevallos, L.; Jacobo-Velázquez, D.A. The Folin–Ciocalteu Assay Revisited: Improvement of Its Specificity for Total Phenolic Content Determination. *Analytical Methods* **2013**, *5*, 5990, doi:10.1039/c3ay41125g.
34. Masyita, A.; Mustika Sari, R.; Dwi Astuti, A.; Yasir, B.; Rahma Rumata, N.; Emran, T. Bin; Nainu, F.; Simal-Gandara, J. Terpenes and Terpenoids as Main Bioactive Compounds of Essential Oils, Their Roles in Human Health and Potential Application as Natural Food Preservatives. *Food Chem X* **2022**, *13*, 100217, doi:10.1016/j.fochx.2022.100217.
35. Saleem, M. Lupeol, a Novel Anti-Inflammatory and Anti-Cancer Dietary Triterpene. *Cancer Lett* **2009**, *285*, 109–115, doi:10.1016/j.canlet.2009.04.033.
36. Ghafari, A.T.; Jahidin, A.H.; Zakaria, Y.; Hazizul Hasan, M. Anti-Inflammatory Effects of *Vitex Trifolia* Leaves Hydroalcoholic Extract against Hydrogen Peroxide(H2O2)- and Lipopolysaccharide (LPS)-Induced Raw 264.7 Cells. *Malaysian Applied Biology* **2022**, *51*, 185–200, doi:10.55230/mabjournal.v51i4.28.
37. Francenia Santos-Sánchez, N.; Salas-Coronado, R.; Villanueva-Cañongo, C.; Hernández-Carlos, B. Antioxidant Compounds and Their Antioxidant Mechanism. In *Antioxidants*; IntechOpen, 2019.
38. Wei, M.; He, X.; Liu, N.; Deng, H. Role of Reactive Oxygen Species in Ultraviolet-Induced Photodamage of the Skin. *Cell Div* **2024**, *19*, 1, doi:10.1186/s13008-024-00107-z.
39. Shahidi, F.; Samarasinghe, A. How to Assess Antioxidant Activity? Advances, Limitations, and Applications of in Vitro, in Vivo, and Ex Vivo Approaches. *Food Production, Processing and Nutrition* **2025**, *7*, 50, doi:10.1186/s43014-025-00326-z.
40. Yusharyahya, S.N. Mekanisme Penuaan Kulit Sebagai Dasar Pencegahan Dan Pengobatan Kulit Menua. *eJournal Kedokteran Indonesia* **2021**, *9*, 150, doi:10.23886/ejki.9.49.150.
41. Pientaweeratch, S.; Panapisal, V.; Tansirikongkol, A. Antioxidant, Anti-Collagenase and Anti-Elastase Activities of *Phyllanthus Emblica* , *Manilkara Zapota* and Silymarin: An *in Vitro* Comparative Study for Anti-Aging Applications. *Pharm Biol* **2016**, *54*, 1865–1872, doi:10.3109/13880209.2015.1133658.
42. Sin, B.Y.; Kim, H.P. Inhibition of Collagenase by Naturally-Occurring Flavonoids. *Arch Pharm Res* **2005**, *28*, 1152–1155, doi:10.1007/BF02972978.

 doi:10.20944/preprints202511.1814.v1

43. Masaki, H. Role of Antioxidants in the Skin: Anti-Aging Effects. *J Dermatol Sci* **2010**, *58*, 85–90, doi:10.1016/j.jdermsci.2010.03.003.
44. Mondal, H.; Thomas, J.; Amaresan, N. Cytotoxicity Assay. In; 2023; pp. 191–193.
45. McCarty, M.F.; Contreras, F. Increasing Superoxide Production and the Labile Iron Pool in Tumor Cells May Sensitize Them to Extracellular Ascorbate. *Front Oncol* **2014**, *4*, doi:10.3389/fonc.2014.00249.
46. Klingelhoeffer, C.; Kämmerer, U.; Koospal, M.; Mühling, B.; Schneider, M.; Kapp, M.; Kübler, A.; Germer, C.-T.; Otto, C. Natural Resistance to Ascorbic Acid Induced Oxidative Stress Is Mainly Mediated by Catalase Activity in Human Cancer Cells and Catalase-Silencing Sensitizes to Oxidative Stress. *BMC Complement Altern Med* **2012**, *12*, 61, doi:10.1186/1472-6882-12-61.
47. Sestili, P.; Brandi, G.; Brambilla, L.; Cattabeni, F.; Cantoni, O. Hydrogen Peroxide Mediates the Killing of U937 Tumor Cells Elicited by Pharmacologically Attainable Concentrations of Ascorbic Acid: Cell Death Prevention by Extracellular Catalase or Catalase from Cocultured Erythrocytes or Fibroblasts. *J Pharmacol Exp Ther* **1996**, *277*, 1719–1725.
48. Garbi, M.I.; Osman, E.E.; Kabbashi, A.S.; Saleh, M.S.; Yousof, Y.S.; Mahmoud, S.A.; Salam, H.A. Cytotoxicity of *Vitex Trifolia* Leaf Extracts On Mcf-7 and Vero Cell Lines. *International Research Journal of Natural Sciences* **2017**, *4*, 89–93.
49. Wee, H.-N.; Neo, S.-Y.; Singh, D.; Yew, H.-C.; Qiu, Z.-Y.; Tsai, X.-R.C.; How, S.-Y.; Yip, K.-Y.C.; Tan, C.-H.; Koh, H.-L. Effects of *Vitex Trifolia* L. Leaf Extracts and Phytoconstituents on Cytokine Production in Human U937 Macrophages. *BMC Complement Med Ther* **2020**, *20*, 91, doi:10.1186/s12906-020-02884-w.
50. Zhu, J.; Li, G.; Zhou, J.; Xu, Z.; Xu, J. Cytoprotective Effects and Antioxidant Activities of Acteoside and Various Extracts of Clerodendrum Cyrtophyllum Turcz Leaves against T-BHP Induced Oxidative Damage. *Sci Rep* **2022**, *12*, 12630, doi:10.1038/s41598-022-17038-w.
51. Marais, T.L. Des; Kluz, T.; Xu, D.; Zhang, X.; Gesumaria, L.; Matsui, M.S.; Costa, M.; Sun, H. Transcription Factors and Stress Response Gene Alterations in Human Keratinocytes Following Solar Simulated Ultra Violet Radiation. *Sci Rep* **2017**, *7*, 13622, doi:10.1038/s41598-017-13765-7.
52. Guo, K.; Liu, R.; Jing, R.; Wang, L.; Li, X.; Zhang, K.; Fu, M.; Ye, J.; Hu, Z.; Zhao, W.; et al. Cryptotanshinone Protects Skin Cells from Ultraviolet Radiation-Induced Photoaging via Its Antioxidant Effect and by Reducing Mitochondrial Dysfunction and Inhibiting Apoptosis. *Front Pharmacol* **2022**, *13*, doi:10.3389/fphar.2022.1036013.
53. Gao, S.; Guo, K.; Chen, Y.; Zhao, J.; Jing, R.; Wang, L.; Li, X.; Hu, Z.; Xu, N.; Li, X. Keratinocyte Growth Factor 2 Ameliorates UVB-Induced Skin Damage via Activating the AhR/Nrf2 Signaling Pathway. *Front Pharmacol* **2021**, *12*, doi:10.3389/fphar.2021.655281.
54. Savini, I.; D'Angelo, I.; Ranalli, M.; Melino, G.; Avigliano, L. Ascorbic Acid Maintenance in HaCaT Revents Radical Formation and Apoptosis by UV-B. *Free Radic Biol Med* **1999**, *26*, 1172–1180, doi:10.1016/S0891-5849(98)00311-6.
55. Erika Chriscensia; Joshua Nathanael; Urip Perwitasari; Agus Budiawan Naro Putra; Shakila Angjaya Adiyanto; Pietradewi Hartrianti Potential Utilisation of *Theobroma Cacao* Pod Husk Extract: Protective Capability Evaluation Against Pollution Models and Formulation into Niosomes. *Trop Life Sci Res* **2024**, *35*, 107–140, doi:10.21315/tlsr2024.35.2.6.
56. Widiatmoko, A.; Fitri, L.E.; Endharti, A.T.; Murlistyarini, S.; Brahmanti, H.; Yuniaswan, A.P.; Ekasari, D.P.; Rasyidi, F.; Nahlia, N.L.; Safitri, P.R. Inhibition Effect of Physalis Angulata Leaf Extract on Viability, Collagen Type I, and Tissue Inhibitor of Metalloproteinase 1 (TIMP-1) but Not Plasminogen Activator Inhibitor-1 (PAI-1) of Keloid Fibroblast Culture. *Clin Cosmet Investig Dermatol* **2023**, *Volume 16*, 2365–2373, doi:10.2147/CCID.S425036.
57. Calvo, M.J.; Navarro, C.; Durán, P.; Galan-Freyle, N.J.; Parra Hernández, L.A.; Pacheco-Londoño, L.C.; Castelanich, D.; Bermúdez, V.; Chacin, M. Antioxidants in Photoaging: From Molecular Insights to Clinical Applications. *Int J Mol Sci* **2024**, *25*, 2403, doi:10.3390/ijms25042403.
58. Kwon, K.-R.; Alam, M.B.; Park, J.-H.; Kim, T.-H.; Lee, S.-H. Attenuation of UVB-Induced Photo-Aging by Polyphenolic-Rich Spatholobus Suberectus Stem Extract Via Modulation of MAPK/AP-1/MMPs Signaling in Human Keratinocytes. *Nutrients* **2019**, *11*, 1341, doi:10.3390/nu11061341.

 doi:10.20944/preprints202511.1814.v1

59. Mu, J.; Ma, H.; Chen, H.; Zhang, X.; Ye, M. Luteolin Prevents UVB-Induced Skin Photoaging Damage by Modulating SIRT3/ROS/MAPK Signaling: An in Vitro and in Vivo Studies. *Front Pharmacol* **2021**, *12*, doi:10.3389/fphar.2021.728261.
60. Nowak-Perlak, M.; Olszowy, M.; Woźniak, M. The Natural Defense: Anti-Aging Potential of Plant-Derived Substances and Technological Solutions Against Photoaging. *Int J Mol Sci* **2025**, *26*, 8061, doi:10.3390/ijms26168061.
61. Mir, H.A.; Ali, R.; Wani, Z.A.; Khanday, F.A. Pro-Oxidant Vitamin C Mechanistically Exploits P66Shc/Rac1 GTPase Pathway in Inducing Cytotoxicity. *Int J Biol Macromol* **2022**, *205*, 154–168, doi:10.1016/j.ijbiomac.2022.02.046.